

Hybrid con guration content of heavy S-wave mesons

Tommy Burd¹ and Doug Toussaint²

(MILC Collaboration)

¹ Institut für Theoretische Physik, Universität Regensburg, D-93040 Regensburg, Germany

² Department of Physics, University of Arizona, Tucson, AZ 85721, USA.

(Dated: December 24, 2018)

We use the non-relativistic expansion of QCD (NRQCD) on the lattice to study the lowest hybrid con guration contribution to the ground state of heavy S-wave mesons. Using lowest-order lattice NRQCD to create the heavy-quark propagators, we form a basis of "unperturbed" S-wave and hybrid states. We then apply the lowest-order coupling of the quark spin and chromomagnetic field at an intermediate time slice to create "mixed" correlators between the S-wave and hybrid states. From the resulting amplitudes, we extract the off-diagonal element of our two-state Hamiltonian. Diagonalizing this Hamiltonian gives us the admixture of hybrid con guration within the meson ground state. The present work represents a continuation of previous work: the analysis has been extended to include lattices of varying spacings, source operators having better overlap with the ground states, and the pseudoscalar (along with the vector) channel. Results are presented for bottomonium ($J^P = 1^+$) using three different sets of quenched lattices. We also show results for charmonium ($J^P = 1^+$) from one lattice set, although we note that the non-relativistic approximation is not expected to be very good in this case.

PACS numbers: 11.15.Ha, 12.38.Gc

I. INTRODUCTION

The existence of valence gluons in bound quark systems, a theoretical possibility considered for a long time in QCD, continues to elude confirmation. Allowance for gluonic excitations increases the range of possible hadronic quantum numbers (J^P) beyond those predicted by constituent quark models. Exotic states should appear (for a recent review see [1]) and, in fact, one such state (1^+) has been observed recently [2], but the underlying structure of the state (hybrid meson, four-quark state, meson molecule, etc.) has not been determined. When considering gluonic constituents, however, the resulting state need not be exotic; the valence gluons may also combine with the quarks and antiquarks to form a state which may otherwise be formed without the gluonic presence. In this non-exotic scenario, a meson (or baryon) state should consist of a mixture of configurations; not only the case where only the valence quarks and antiquarks appear, but also those where a gluonic excitation is present: a hybrid con guration.

As a relevant example (since this is one of the systems we study in the present work) we may look at the vector meson state for bottomonium (1^+). We may envision the ground state for this system as a bottom quark and antiquark in a color singlet, a relative S-wave, and a spin triplet. However, the true ground state should also have a contribution where the quark and antiquark are in a spin singlet and a color octet, the spin of the meson and the overall color singlet being ensured by the gluonic excitation:

$$\begin{aligned} j^i &= A_s j_{bi} + A_h j_{bg}i \\ &= \cos \theta j_S(1^-)i + \sin \theta j_H(1^-)i; \end{aligned} \quad (1)$$

It is just this type of (albeit simplified) two-state system

we consider in the present work. We also consider the 0^+ heavy S-wave meson:

$$j^i = \cos \theta j_S(0^+)i + \sin \theta j_H(0^+)i; \quad (2)$$

Hybrid-quarkonium con guration mixing has been considered before in the framework of the MIT bag model [3, 4] and with the use of an adiabatic potential model [5]. We compare results from this on-going lattice work [6, 7, 8] with these previous results.

II. LATTICE METHOD

We work in the heavy-quark limit, so we use the non-relativistic expansion of lattice QCD [9, 10, 11]. To evolve our quark propagators we use a time-step-symmetric form for the transfer matrix [6, 12]:

$$(x; t+a) = \left(1 - \frac{aH_0}{2n} \right)_{t+a}^n U_4^y(x) \left(1 - \frac{aH_0}{2n} \right)_t^n (1 - t^0; t^0; a H) (x; t); \quad (3)$$

The Hamiltonian applied at all time slices, H_0 , accounts for the kinetic energy of the heavy quarks:

$$H_0 = \frac{q^2}{2m_q}; \quad (4)$$

where the q^2 is the lattice covariant Laplacian. At one intermediate time slice, t^0 , the lowest-order spin-dependent interaction,

$$H = g \frac{q}{2m_q} \sim B; \quad (5)$$

is applied, thereby allowing a spin \mathbf{ip} of the quark (or antiquark) in exchange for the emission or absorption of a gluonic excitation; i.e., con guration mixing.

The local value of the chromomagnetic field is calculated using the clover formulation, averaging the fields generated from the four plaquettes surrounding a lattice site:

$$\begin{aligned} \langle \mathbf{x} \rangle = & \frac{1}{4} \mathbf{U} \langle \mathbf{x} \rangle \mathbf{U} \langle \mathbf{x} + \hat{\mathbf{x}} \rangle \mathbf{U}^Y \langle \mathbf{x} + \hat{\mathbf{x}} \rangle \mathbf{U}^Y \langle \mathbf{x} \rangle \\ & + \mathbf{U} \langle \mathbf{x} \rangle \mathbf{U}^Y \langle \mathbf{x} + \hat{\mathbf{x}} \rangle \mathbf{U}^Y \langle \mathbf{x} - \hat{\mathbf{x}} \rangle \mathbf{U} \langle \mathbf{x} - \hat{\mathbf{x}} \rangle \\ & + \mathbf{U}^Y \langle \mathbf{x} - \hat{\mathbf{x}} \rangle \mathbf{U}^Y \langle \mathbf{x} - \hat{\mathbf{x}} \rangle \mathbf{U} \langle \mathbf{x} + \hat{\mathbf{x}} \rangle \mathbf{U} \langle \mathbf{x} + \hat{\mathbf{x}} \rangle \\ & + \mathbf{U}^Y \langle \mathbf{x} - \hat{\mathbf{x}} \rangle \mathbf{U} \langle \mathbf{x} - \hat{\mathbf{x}} \rangle \mathbf{U} \langle \mathbf{x} + \hat{\mathbf{x}} \rangle \mathbf{U}^Y \langle \mathbf{x} \rangle ; \quad (6) \end{aligned}$$

$$F \langle \mathbf{x} \rangle = \frac{1}{2i} \langle \mathbf{x} \rangle - \langle \mathbf{x} \rangle^Y - \frac{1}{3} \text{Im} [\Gamma \mathbf{r} \langle \mathbf{x} \rangle] : \quad (7)$$

The chromomagnetic field arises from the spatial components,

$$F_{jk} \langle \mathbf{x} \rangle = "j_{jk} g B_1 \langle \mathbf{x} \rangle : \quad (8)$$

Tadpole improvement [13] is also included, the factor u_0 being calculated via the average plaquette and applied to all the link variables:

$$\mathbf{U} \langle \mathbf{x} \rangle = \frac{\mathbf{U} \langle \mathbf{x} \rangle}{u_0} ; \quad F \langle \mathbf{x} \rangle = \frac{F \langle \mathbf{x} \rangle}{u_0^4} : \quad (9)$$

Creating the heavy-quark propagators with this form for the evolution operator, we then use appropriate operators at the source and sink time slices to project out the desired meson states. The heavy-meson operators we use, along with the corresponding quantum numbers, may be found in Table 1 of Ref. [6].

Two different types of quark sources are used: a random wall (RW) and a Coulomb-gauge-fixed wall (CW). The RW source is an incoherent collection of point sources, the average meson propagator having contributions only from where the quark and antiquark start at the same location. The CW source provides a "maximally smeared" source, with contributions from spatially separated quarks and antiquarks. In both cases, the sink end is simply a sum over points where both the quark and antiquark coexist.

We fit the S-wave propagator with the following form:

$$C_s(t) = A_{1s} e^{m_{1s}t} + A_{2s} e^{m_{2s}t} ; \quad (10)$$

allowing a determination of the 2S-1S mass splitting. We also have P-wave correlators, which we fit (at least for the CW source) with only a single mass,

$$C_p(t) = A_{2p} e^{m_{2p}t} : \quad (11)$$

We use the 2P-1S mass splitting to set the lattice scale. A single mass t is also used for the hybrid correlators,

$$C_h(t) = A_{1h} e^{m_{1h}t} : \quad (12)$$

After application of the spin-dependent term in the Hamiltonian at t^0 (or t^{00}), a signal appears for the "mixed" correlator, hybrid ! S-wave (or vice versa). We fit these correlators in the region $t > t^0$ (or $t > t^{00}$) with the form s:

$$C_{hs}^{(1)}(t^0; t) = A_{1hs}(t^0) e^{m_{1s}(t - t^0)} \quad (13)$$

and

$$C_{sh}^{(1)}(t^{00}; t) = A_{1sh}(t^{00}) e^{m_{1h}(t - t^{00})} : \quad (14)$$

Looking more closely at the amplitude for the first correlator (hybrid ! S-wave), we can reason that there should be factors from the overlap of the source operator with the hybrid, the overlap of the sink operator with the S-wave, the exponential decay of the hybrid state before t^0 , and the matrix element with which we are interested:

$$A_{1hs}(t^0) = A_{1h}^{1=2} A_{1s}^{1=2} \langle \mathbf{h} \mathbf{l} \mathbf{S} | \mathbf{H} | \mathbf{j} \mathbf{l} \mathbf{H} \rangle e^{m_{1h}t^0} : \quad (15)$$

Knowing the masses and amplitudes from the standard S-wave and hybrid correlators, we solve for the off-diagonal matrix element of our two-state Hamiltonian. This is repeated for larger values of t^0 to find a plateau in the final result, where we may be sure that only the ground-state contribution from the source appears. A similar procedure may be followed for the S-wave ! hybrid correlator.

There is a complication, however, which arises for our CW-source correlators: the operators at the source and sink ends are not the same. At one end we have a Coulomb-gauge-fixed wall (cw) source, while at the other end there is a point (p) sink. The amplitude for the S-wave correlator therefore has the form

$$A_{1s} = A_{1s_{cw}}^{1=2} A_{1s_p}^{1=2} ; \quad (16)$$

while that for the hybrid is

$$A_{1h} = A_{1h_{cw}}^{1=2} A_{1h_p}^{1=2} : \quad (17)$$

From each of these products, the mixed correlators include only one of the factors (rather than just the square root of each amplitude):

$$A_{1hs}(t^0) = A_{1s_p}^{1=2} A_{1h_{cw}}^{1=2} \langle \mathbf{h} \mathbf{l} \mathbf{S} | \mathbf{H} | \mathbf{j} \mathbf{l} \mathbf{H} \rangle e^{m_{1h}t^0} \quad (18)$$

and

$$A_{1sh}(t^{00}) = A_{1h_p}^{1=2} A_{1s_{cw}}^{1=2} \langle \mathbf{h} \mathbf{l} \mathbf{H} | \mathbf{H} | \mathbf{j} \mathbf{l} \mathbf{S} \rangle e^{m_{1s}t^{00}} : \quad (19)$$

In order to get the appropriate cancellations of amplitudes, we thus need to use a geometric mean:

$$\langle \mathbf{j} \mathbf{l} \mathbf{S} | \mathbf{H} | \mathbf{j} \mathbf{l} \mathbf{H} \rangle ij = \frac{A_{1hs}(t^0) A_{1sh}(t^{00})}{A_{1s} A_{1h}} e^{m_{1h}t^0} e^{m_{1s}t^{00}} \quad (20)$$

at large t^0, t^{00} .

We average the correlators over sets of quenched lattices, generated using a Symanzik 1-loop improved gauge

TABLE I: Quenched NRQCD runs.

N_s^3	N_t	u_0	am_q	n	sources	# con gs.
7.75	16^3	32	0.8800	3.2, 3.6	2 RW, CW	220
8.00	20^3	64	0.8879	2.5, 2.8	2 RW, CW	240
∞	∞	∞	$0.7, 0.8$	3	CW	170
8.40	28^3	96	0.89741	1.8, 2.0	2 RW, CW	76

action [13, 14, 15, 16, 17]. The relevant parameters for these runs are listed in Table I.

To set the physical scale for the lattice spacing and determine the physical quark mass, we use the same procedure as was used previously for bottomonium spectroscopy with NRQCD [18]. For the lattice spacings, we use bottomonium mass splittings, such as the spin-averaged 2P-1S mass difference ($M_b - M_s = 440$ MeV) and the 2S-1S difference for the ($M_b - M_s = 563$ MeV). We also create non-zero-momentum S-wave correlators and use the resulting dispersion relations to determine the kinetic masses of the ground states. Using the results from two quark masses, an interpolation (or extrapolation) may be made to match the kinetic S-wave mass to that of the ($M_b = 946$ GeV), thus arriving at a physical bottom quark mass.

In an attempt to determine the radiative correction c_B , we also create correlators with the spin-dependent term applied at all intermediate time slices and with the values of $c_B = 1$ and 2. We then determine the resulting S-wave hyperfine splittings, which to lowest order should be quadratic in this term: $m_{1s}(1) - m_{1s}(0^+) / c_B^2$. There is, however, a danger in assuming this to be the only (or the largest) contribution to the hyperfine splitting: previous investigations of quarkonium spin-dependent splittings in lattice NRQCD [19, 20] display significant contributions from various $O(v^4)$ and $O(v^6)$ terms in the velocity expansion (and poor convergence of this expansion for cc systems). Therefore, a value of c_B (a) determined in this way includes not only the desired radiative correction, but also systematic effects due to the neglect of other relativistic terms in the NRQCD expansion. To further complicate the matter, the 0^+ bottomonium state (b) has yet to be observed experimentally.

III. RESULTS

The Coulomb-gauge-fixed wall (CW) sources provide good overlap with the desired meson states and reasonable t s are obtained earlier than for the random wall (RW) sources. Figure 1 displays one set of t masses for the S-wave, P-wave (0^{++}), and hybrid (0^+) correlators versus the minimum time chosen for each t . A complete list of the t s used for our results, along with the amplitudes, masses, and χ^2 values may be found in Ref. [8].

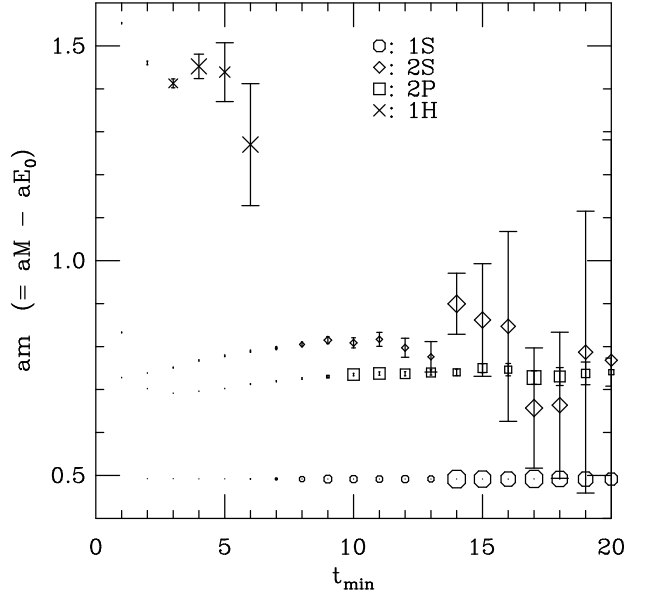


FIG. 1: 0^+ t masses versus the minimum time used for the t s. $a = 8.0$, $am_q = 2.5$, CW source. The size of the symbol is proportional to the confidence of the t (the symbols in the legend represent 50% confidence).

The results for the lattice spacings are presented in Table II, along with other determinations from the static-quark potential using a modified Sommer parameter r_0 [21, 22] and the string tension σ . Looking at the NRQCD results, we are encouraged by the consistency (within the errors) of the 2P-1S and 2S-1S mass splittings. We would like to point out, however, that our heavy-quark Hamiltonian leaves out many terms in the relativistic expansion and, for this reason, we do not claim to be presenting a very precise determination of the bottomonium spectrum; this has been studied by others using more elaborate forms of lattice NRQCD [18, 23]. There are marked differences between the lattice spacings determined via the bottomonium mass splittings and those from the static quark potentials; in fact, the two static-quark determinations disagree. The string-tension results consistently give the largest lattice spacings (a in fm), while the bottom mass splittings give the smallest. The main reason for the difference of these two extremes appears to be the quenched approximation. A comparison of the static-quark potentials for quenched and dynamical configurations [22] has shown that, in the quenched case, the potentials do not display sufficient curvature: the Coulomb-like potential well at short distances is not as deep as in the dynamical case and the linear string-like region is steeper. This should lead to an underestimation of the bottom mass splittings in lattice units since these systems are relatively small. This would seem to explain the low values for the lattice spacings seen in Table II. The string-tension results are thus expected to give the larger lattice spacings for the quenched lattices. A cursory study using the Born-Oppenheimer approximation

TABLE II: Lattice spacing determinations with $c_B = 0$, CW source. Physical scales used: $r_1 = 0.344$ fm ; $a^{1=2} = 440$ MeV ; $M_b M_c = 440$ MeV ; $M_b M_c = 563$ MeV . The * denote values used for a throughout this work .

am _q	physical scale	a ¹ (MeV)
7.75	1 $r_1 = a = 2.095(13)$	1200(7)
	1 $a^2 = 0.1652(47)$	1082(15)
	3.2 $a(M_b M_c) = 0.328(13)$	1341(53)*
	3.6 $a(M_b M_c) = 0.324(12)$	1358(51)
	3.2 $a(M_b M_c) = 0.487(60)$	1160(140)
	3.6 $a(M_b M_c) = 0.434(34)$	1300(100)
8.00	1 $r_1 = a = 2.6580(58)$	1522(3)
	1 $a^2 = 0.09955(10)$	1394(7)
	2.5 $a(M_b M_c) = 0.2456(42)$	1792(31)*
	2.8 $a(M_b M_c) = 0.2431(40)$	1811(30)
	2.5 $a(M_b M_c) = 0.3233(88)$	1742(48)
	2.8 $a(M_b M_c) = 0.3131(73)$	1797(43)
8.40	1 $r_1 = a = 3.7301(69)$	2136(4)
	1 $a^2 = 0.04989(46)$	1970(9)
	1.8 $a(M_b M_c) = 0.1749(50)$	2516(71)*
	2.0 $a(M_b M_c) = 0.1724(47)$	2552(69)
	1.8 $a(M_b M_c) = 0.235(16)$	2400(160)
	2.0 $a(M_b M_c) = 0.229(14)$	2460(140)

TABLE III: Kinetic masses for the 1S states and the resulting (lattice-regularized) physical quark masses. The lattice scale is set using the spin-averaged 2P-1S mass differences found for the bb system s.

am _q	aM _{1S} ^{kin}	M _{1S} ^{kin} (GeV)	am _b	m _b (GeV)
7.75	3.2 7.38(54)	9.90(72)	3.09(21)	4.17(28)
	3.6 8.44(59)	11.46(80)		
8.0	2.5 5.509(77)	9.87(14)	2.41(4)	4.34(7)
	2.8 6.178(90)	11.19(16)		
8.4	1.8 4.00(16)	10.06(40)	1.70(7)	4.31(18)
	2.0 4.42(17)	11.28(43)		
	am _c	m _c (GeV)		
8.0	0.7 1.752(23)	3.154(41)	0.677(12)	1.219(22)
	0.8 1.964(26)	3.535(47)		

[8] supports these claims.) In the spirit of presenting a self-consistent work, however, we use the lattice spacings provided by the 2P-1S bottomonium mass splittings.

In Table III we present our results for the 1S kinetic masses determined from the dispersion relations:

$$E_{1S}(p) = \frac{p^2}{2M_{1S}^{kin}} + m_{1S} : \quad (21)$$

Each case requires an extrapolation in quark mass to reach the physical value $M_{1S}^{kin} = M_c = 9.46$ GeV .

As described in the previous section, we use the amplitudes from the mixed correlators, along with the masses

and amplitudes from the "unmixed" ones, to determine the off-diagonal element of our two-state Hamiltonian. Figures 2-5 show the results for these matrix elements as functions of the time, t^0 , at which the spin-dependent term is applied to the heavy-quark propagators. The CW -source results each have the remaining factor of

$$\frac{A_{1s_p}^{1=2} A_{1h_{cw}}^{1=2}}{A_{1s}^{1=2} A_{1h}^{1=2}} = \frac{A_{1s_p}^{1=4} A_{1h_{cw}}^{1=4}}{A_{1s_{cw}}^{1=4} A_{1h_p}^{1=4}} = \frac{A}{A_{rev}}^{1=2} \quad (22)$$

(or its reciprocal) which requires the use of a geometric mean (see Eq. 20) to ensure its removal. The results chosen for the final geometric means are displayed with dotted symbols. All errors result from a single-elimination jackknife routine.

Figure 2 displays results for the configuration-mixing matrix element from one set of lattices ($= 8.0$) and one value of the quark mass ($am_q = 2.5$). Results are shown using both the CW and RW sources. The hybrid correlators for the latter, however, have their masses fixed to the values found from the CW -source hybrid correlators since these provide more reliable mass plateaus. The two horizontal lines show the 1 limits for the geometric mean of the CW -source results. The hybrid! S-wave results do not display very convincing plateaus, especially for the 1 channel. However, within the errors, the final results are consistent with the plateaus from the RW source. These results appear to be about 30% lower than previous determinations using only the RW sources [6, 7], thereby stressing the need for reliable hybrid mass determinations, which the CW -source correlators more readily provide.

Figures 3 and 4 display similar plots for the $= 7.75$ and 8.4 lattices, respectively. Here we see more convincing plateaus for the matrix element from the hybrid! S-wave correlators.

In Fig. 5 we show the results for one of the lighter masses (around m_c) for the $= 8.0$ lattices. A quick look at the result for the 1 channel, however, shows that the non-relativistic approximation (at least at the level of simplicity in our heavy-quark Hamiltonian) may not be such a great idea:

$$\frac{hH_j H_j S_i}{2m_q} \frac{0.14}{1.4} 0.1 v^4 : \quad (23)$$

In spite of this we carry on and present our results for charmonium, encouraging the reader not to forget the large systematic effect we may have introduced by neglecting other terms in our heavy-quark Hamiltonian.

All of the CW -source results for the configuration-mixing matrix elements, along with the corresponding mixing angles, are shown in Tables IV and V . The last column displays the final results after an extrapolation (linear) in quark mass to the bottom (or charm) mass determined previously (see Table III). The hybrid configuration content of the 0^-_p ground state is enhanced by the expected factor of $\sqrt{3}$ (due to spin statistics for

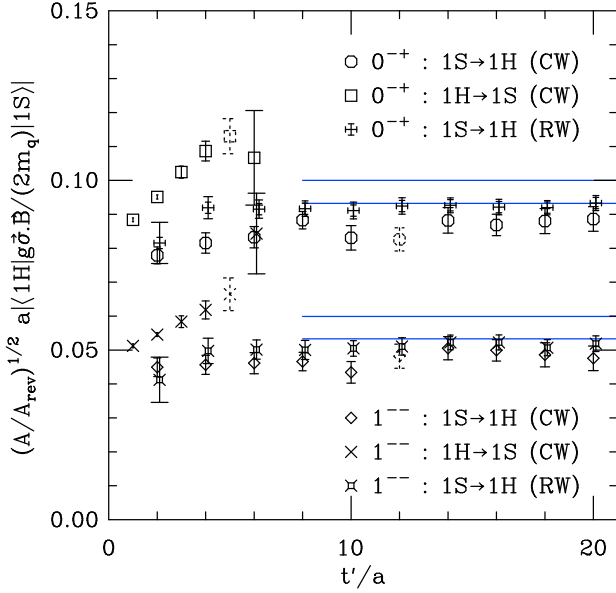


FIG. 2: Comparison of the results obtained for the mixing matrix element via the CW source and the RW source with the hybrid mass fixed to that found with the CW hybrid source. The dotted symbols mark the ones used in the geometric mean to get the CW source results, the 1 ranges of which are denoted by the horizontal lines.

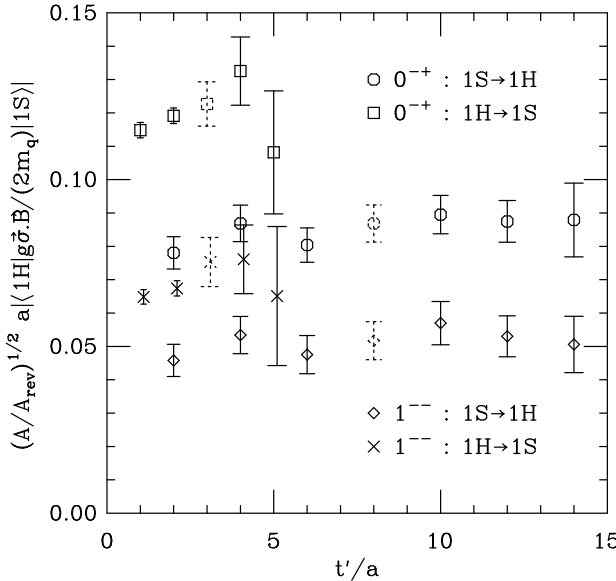


FIG. 3: The mixing matrix element vs the time of application of the interaction term. CW source, $\gamma = 7.75$, $am_q = 3.2$. The dotted symbols mark the ones used in the geometric mean to get the CW source results.

single-gluon emission/absorption [3, 24]) relative to that in the 1^- channel. Up to this point we have ignored the radiative correction ($c_B = 1$) and we point out the need for this factor, c_B ($\langle \rangle$), in the final column. To be precise, this factor should be included in the mixing matrix element, but for small mixing angles, this correc-

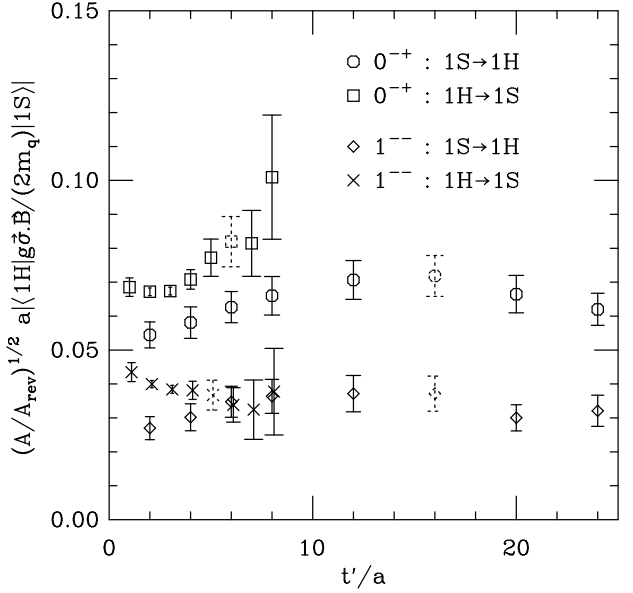


FIG. 4: The mixing matrix element vs the time of application of the interaction term. CW source, $\gamma = 8.4$, $am_q = 1.8$. The dotted symbols mark the ones used in the geometric mean to get the CW source results.

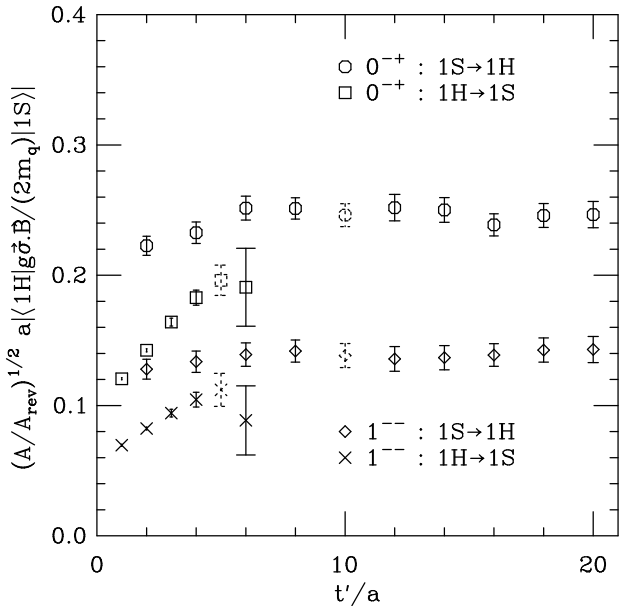


FIG. 5: The mixing matrix element vs the time of application of the interaction term. CW source, $\gamma = 8.0$, $am_q = 0.7$. The dotted symbols mark the ones used in the geometric mean to get the CW source results.

tion appears as a multiplicative factor in the final result: $\sin \pi m_{1H} j_1 \sin \pi m_{1S} j_2$.

Meson correlators with the $\sim B$ term applied at all intermediate time slices were also created in order to study the S-wave hyperfine splittings and to attempt to determine c_B ($\langle \rangle$). For these, the values of $c_B = 1$ and 2 were intended; however, a sign error was discovered

TABLE IV : Results for the 1^- S-wave/hybrid configuration mixing (CW source).

am_q	$j1H$	j_1H	$j1Sij$	$j\sin(\theta)j$	$j1H j_{ij}$
7.75	3.2	0.0624 (61)	0.0566 (27)	0.058 (3)	$c_B(=)$
	3.6	0.0582 (61)	0.0518 (27)		
8.0	2.5	0.0566 (33)	0.0618 (28)	0.063 (3)	$c_B(=)$
	2.8	0.0522 (31)	0.0564 (27)		
8.4	1.8	0.0369 (44)	0.0618 (36)	0.064 (4)	$c_B(=)$
	2.0	0.0352 (44)	0.0578 (36)		
			$j1H j_{j=ij}$		
8.0	0.7	0.1349 (84)	0.1483 (81)	0.150 (8)	$c_B(=)$
	0.8	0.1259 (74)	0.1393 (70)		

TABLE V : Results for the 0^+ S-wave/hybrid configuration mixing (CW source).

am_q	$j1H$	j_1H	$j1Sij$	$j\sin(\theta)j$	$j1H j_{bij}$
7.75	3.2	0.1032 (58)	0.0945 (26)	0.097 (3)	$c_B(=)$
	3.6	0.0954 (57)	0.0862 (26)		
8.0	2.5	0.0966 (34)	0.1031 (29)	0.106 (3)	$c_B(=)$
	2.8	0.0887 (32)	0.0939 (27)		
8.4	1.8	0.0767 (60)	0.1156 (52)	0.120 (5)	$c_B(=)$
	2.0	0.0723 (61)	0.1074 (53)		
			$j1H j_{cij}$		
8.0	0.7	0.2327 (77)	0.2403 (62)	0.243 (6)	$c_B(=)$
	0.8	0.2172 (69)	0.2270 (56)		

(much too late) in our field-strength routine which forces us to work with $c_B = 1$ and 2. (This has no effect upon our configuration-mixing results up to this point since they result from a single application of the spin-dependent term.) The resulting hyperfine splittings for the S-wave states may be found in Table VI.

Whereas our bottomonium systems seem to follow the c_B^2 proportionality and our charmonium systems do not, there is no experimentally measured mass for the 0^+

TABLE VI: 1S hyperfine splittings.

am_q	c_B^2	M_b	M_c	$(M_b - M_c) \text{ (MeV)}$	$c_B^2(=)$
7.75	3.2	1	16.7 (1.3)	(M)	$M_b - M_c = (17 \text{ MeV})$
		4	63.6 (5.1)		
8.0	2.5	1	21.90 (55)	(M)	$M_b - M_c = (22 \text{ MeV})$
		4	81.6 (2.6)		
8.4	1.8	1	25.2 (1.1)	(M)	$M_b - M_c = (25 \text{ MeV})$
		4	93.5 (4.9)		
		$M_{J=}$	M_c	$(M \text{ MeV})$	
8.0	0.7	1	68.0 (1.8)		$1.2 - 1.7$
		4	213.6 (7.1)		

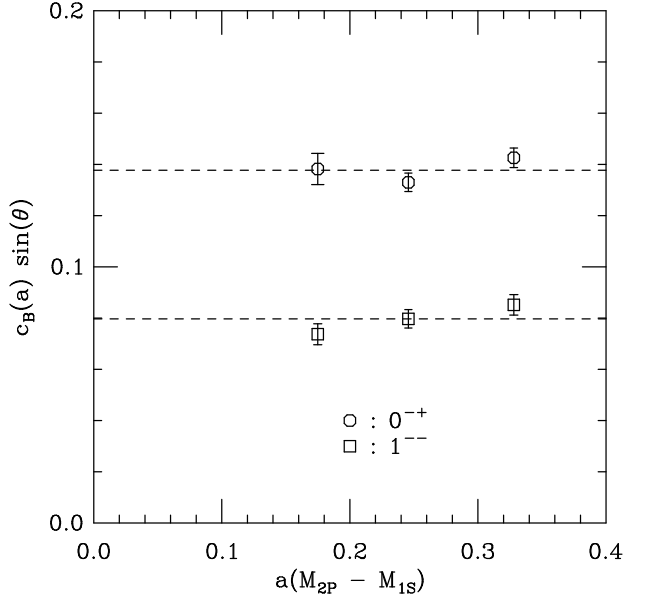


FIG. 6: Hybrid/S-wave configuration mixing angle vs lattice spacing. The radiative correction was set using $M_b = 26 \text{ MeV}$ [$c_B(a) = 1.02; 1.09; 1.24$ from left to right]. The horizontal lines are the averages. They are placed in the figure to show the relatively small dependence of the mixing upon a that we see; they are not meant to imply a continuum extrapolation.

bottomonium (b) while the corresponding charm meson (c) has been observed. So we report our findings for $c_B^2(a)$ from the bottomonium system in terms of the $M_b - M_c$ mass splitting. For the charmonium results, we report two values for $c_B^2(a)$. The larger value is the result of a linear extrapolation from 0 through the $c_B^2 = 1$ point to $M_{J=0} - M_c = 117 \text{ MeV}$ at $c_B^2 = c_B^2(=)$. If we believe the physical quark mass shifts with the inclusion of the spin-dependent term and that this is the dominant effect in explaining why our cc hyperfine splitting is not $/ c_B^2$, then this is the result we would trust more. If, however, we believe there is a c_B^3 correction present and that this is the dominant effect, we should trust the lower value, which results from using an interpolation of the form $a_2 c_B^2 + a_3 c_B^3$ through the $c_B = 1$ and 2 points and extrapolating to 117 MeV in the $c_B > 0$ region. If we use these results with that from $b\bar{b}$ at $a = 8.0$, we find $M_b - M_c = 26 - 38 \text{ MeV}$ and $c_B(=) = 7.75, 1.24, 1.50, c_B(=) = 8.0, 1.09, 1.31, c_B(=) = 8.4, 1.02, 1.23$. We use the smaller values here to determine the configuration mixings for our bottomonium systems displayed in Figure 6 as a function of the lattice spacing. The points show the relatively small lattice-spacing dependence which remains once the 1S $b\bar{b}$ hyperfine splitting is known.

Given our previous worries about our cc results ($v^4 = 0.1$), we also consider the possible range of c_B values using potential model values for the $b\bar{b}$ S-wave hyperfine splittings [25, 26]: 30 – 60 MeV, resulting in $c_B(=) =$

7.75) 1.33 1.88; c_B (= 8.0) 1.17 1.65; c_B (= 8.4) 1.10 1.55; or roughly

$j_{1H} j_{ij}$ 0.076 0.11; $j_{1H} j_{bij}$ 0.13 0.19

and

$j_{1H} j_{ij}$ 0.18 0.25; $j_{1H} j_{cij}$ 0.29 0.4;

Each of these ranges lies between two corresponding values (with and without the color Coulomb interaction) determined within the MIT bag model [3]. The upper limit of the $J=$ result is consistent with that from an adiabatic potential model [5].

Again, however, these determinations of c_B () most likely include systematic effects due to the neglect of other terms in the velocity expansion which also contribute to the hyperfine splittings [19, 20]. For this reason, we think it best to be conservative with our estimate and use the lower values reported above: c_B^2 (= 8.0) 1.2.

IV. CONCLUSIONS

We have determined the relative contribution of the lowest hybrid configuration to the wavefunctions of heavy S-wave mesons. Our approach utilizes the non-relativistic approximation to lattice QCD, applicable for heavy quarkonia where there is a clear separation of radial, orbital, and gluonic excitations and the mixing among the corresponding configurations is small.

Adpole-improved, tree-level results ($c_B = 1$ in Tables IV and V) display hybrid configuration admixtures at about $(0.063)^2$ 0.4% probability within the and about $(0.15)^2$ 2.3% for $J=$. The corresponding results for the pseudoscalar channels are enhanced by 3 due to spin statistics [3, 24].

Although the radiative correction for the spin-dependent term in our heavy-quark Hamiltonian provides the largest uncertainty in our calculation, this factor appears to provide further enhancement of the configuration mixing (20% for the probabilities at = 8.0).

Quenching appears to significantly affect the lattice spacing results (see Table II and Ref. [22]), decreasing those determined via bottomonium mass splittings (by perhaps 10%, see Ref. [8]). This, in turn, affects the quark mass extrapolation and the determination of the radiative correction, but the direct effect upon the configuration mixings is not clear. This may only be answered by repeating the analysis on lattices with dynamical quarks.

These results have implications for theoretical determinations of certain quarkonium quantities. For exam-

ple, since the $J=$! e^+e^- decay should not occur directly from the hybrid configuration [27], our results suggest about a 1.2 $(0.15)^2$ 2.7(3)% suppression of the $(J=$! e^+e^-) partial width determined via potential models; about a 1.2 $(0.063)^2$ 0.48(5)% suppression for $($! e^+e^-). These effects appear to be rather small (the corresponding experimental errors lie at about 7% and 4% for $J=$ and , respectively [28]) and this analysis lends support to their neglect thus far.

The other side to this issue is that of the vector hybrid states containing some admixture of the qq vector configurations and therefore coupling to e^+e^- . The above results would suggest the appearance of a cog hybrid resonance with a partial width of

$$(cog ! e^+e^-) \quad 0.027(3) \quad (J= ! e^+e^-) \\ 0.14(2) \text{ keV}$$

somewhere around $E_{cm} = M_{cog}$ 4.4 4.7 GeV (the lower estimate arises from using the r_1 -determined value of the lattice spacing) and a bbq hybrid resonance with

$$(bbq ! e^+e^-) \quad 0.0048(5) \quad (! e^+e^-) \\ 0.0063(7) \text{ keV}$$

around M_{bbq} 10.8 11.1 GeV. Any such bbq-dominated resonance should thus be extremely difficult to see in e^+e^- R-scans given this very small partial width and (most likely) much larger overall width. The cog-dominated state gives a partial width of the same order of that seen in a resonance within the same mass range: (4415) with $(e^+e^-) = 0.47(10)$ keV [28, 29, 30]; (4430) with $(e^+e^-) = 0.390(74)$ keV from Refs. [31, 32]. However, this hardly qualifies as evidence of a hybrid-dominated structure for such a resonance. Any such determination would not only require a study of the possible decays from the hybrid state (determining the total width), but would also need to consider mixings of the cog configuration with other cc configurations which lie closer in mass.

Acknowledgments

This work was supported by the U.S. Department of Energy under contract DE FG03 95ER40906. Computations were performed on Blue Horizon at the San Diego Supercomputing Center and the Nirvana cluster at Los Alamos National Laboratory. We would like to thank Ted Barnes for helpful suggestions.

(2001), [hep-ex/0101058](#).

[3] T. Barnes, *Nucl. Phys. B* 158, 171 (1979).

[4] F. de Viron, *Nucl. Phys. B* 239, 106 (1984).

[5] S. B. Gerasimov (1998), [hep-ph/9812509](#).

[6] T. Burch, K. Orginos, and D. Toussaint, *Phys. Rev. D* 64, 074505 (2001), [hep-lat/0103025](#).

[7] T. Burch, K. Orginos, and D. Toussaint, *Nucl. Phys. Proc. Suppl.* 106, 382 (2002), [hep-lat/0110001](#).

[8] T. Burch (2003), Doctoral Dissertation, Department of Physics, University of Arizona (available at <http://www.physics.arizona.edu/~tburch/>).

[9] W. E. Caswell and G. P. Lepage, *Phys. Lett. B* 167, 437 (1986).

[10] E. Eichten (1987), talk delivered at the Int. Sympos. of Field Theory on the Lattice, Seillac, France, Sep 28–Oct 2, 1987.

[11] G. P. Lepage and B. A. Thacker (1987), presented at Int. Symp. on Quantum Field Theory on the Lattice, Seillac, France, Sep 28–Oct 2, 1987.

[12] G. P. Lepage, L. M. Magnea, C. Nakleh, U. Magnea, and K. Hornbostel, *Phys. Rev. D* 46, 4052 (1992), [hep-lat/9205007](#).

[13] G. P. Lepage and P. B. Mackenzie, *Phys. Rev. D* 48, 2250 (1993), [hep-lat/9209022](#).

[14] K. Symanzik, *Nucl. Phys. B* 226, 187 (1983).

[15] M. Lüscher and P. Weisz, *Phys. Lett. B* 158, 250 (1985).

[16] M. G. Alford, W. Di�m, G. P. Lepage, G. Hockney, and P. B. Mackenzie, *Phys. Lett. B* 361, 87 (1995), [hep-lat/9507010](#).

[17] C. W. Bernard et al. (MILC), *Phys. Rev. D* 58, 014503 (1998), [hep-lat/9712010](#).

[18] C. T. H. Davies et al., *Phys. Rev. D* 50, 6963 (1994), [hep-lat/9406017](#).

[19] H. D. Trottier, *Phys. Rev. D* 55, 6844 (1997), [hep-lat/9611026](#).

[20] C. Stewart and R. Konick, *Phys. Rev. D* 63, 054503 (2001), [hep-lat/0005024](#).

[21] R. Sommer, *Nucl. Phys. B* 411, 839 (1994), [hep-lat/9310022](#).

[22] C. W. Bernard et al., *Phys. Rev. D* 62, 034503 (2000), [hep-lat/0002028](#).

[23] C. T. H. Davies et al. (UKQCD), *Phys. Rev. D* 58, 054505 (1998), [hep-lat/9802024](#).

[24] T. Barnes, F. E. Clos, and F. de Viron, *Nucl. Phys. B* 224, 241 (1983).

[25] Y.-Q. Chen and R. J. Oakes, *Phys. Rev. D* 53, 5051 (1996), [hep-ph/9506377](#).

[26] F. J. Yndurain, *Nucl. Phys. Proc. Suppl.* 93, 196 (2001), [hep-ph/0008007](#).

[27] T. Barnes (2003), personal communication.

[28] K. Hagiwara et al. (Particle Data Group), *Phys. Rev. D* 66, 010001 (2002).

[29] J. Siegrist et al., *Phys. Rev. Lett.* 36, 700 (1976).

[30] R. B. Brandelik et al. (DASP), *Phys. Lett. B* 76, 361 (1978).

[31] J. Z. Bai et al. (BES), *Phys. Rev. Lett.* 88, 101802 (2002), [hep-ex/0102003](#).

[32] M. Eidelman (2002), [hep-ph/0210247](#).